LETTER

doi:10.1038/nature14062

The terrestrial uranium isotope cycle

Morten B. Andersen[1,2], Tim Elliott[1], Heye Freymuth[1], Kenneth W. W. Sims[3], Yaoling Niu[4] & Katherine A. Kelley[5]

Changing conditions on the Earth's surface can have a remarkable influence on the composition of its overwhelmingly more massive interior. The global distribution of uranium is a notable example. In early Earth history, the continental crust was enriched in uranium. Yet after the initial rise in atmospheric oxygen, about 2.4 billion years ago, the aqueous mobility of oxidized uranium resulted in its significant transport to the oceans and, ultimately, by means of subduction, back to the mantle[1–8]. Here we explore the isotopic characteristics of this global uranium cycle. We show that the subducted flux of uranium is isotopically distinct, with high $^{238}U/^{235}U$ ratios, as a result of alteration processes at the bottom of an oxic ocean. We also find that mid-ocean-ridge basalts (MORBs) have $^{238}U/^{235}U$ ratios higher than does the bulk Earth, confirming the widespread pollution of the upper mantle with this recycled uranium. Although many ocean island basalts (OIBs) are argued to contain a recycled component[9], their uranium isotopic compositions do not differ from those of the bulk Earth. Because subducted uranium was probably isotopically unfractionated before full oceanic oxidation, about 600 million years ago, this observation reflects the greater antiquity of OIB sources. Elemental and isotope systematics of uranium in OIBs are strikingly consistent with previous OIB lead model ages[10], indicating that these mantle reservoirs formed between 2.4 and 1.8 billion years ago. In contrast, the uranium isotopic composition of MORB requires the convective stirring of recycled uranium throughout the upper mantle within the past 600 million years.

Recycling of U from the surface to the Earth's deep interior can be monitored by a decrease in the Th/U ratio of the mantle[2–8]. Thorium provides a valuable reference for several reasons. First, U and Th behave similarly as tetravalent species in the mantle, such that they are difficult to fractionate significantly by melting processes. Only under more oxidized surface conditions do the elements show contrasting behaviour, with Th remaining tetravalent and immobile during weathering, unlike highly water-soluble hexavalent U species. Second, both Th and U are refractory, lithophile elements, and so the Th/U of the silicate Earth can be estimated from measurements of meteorites. This planetary Th/U reference has recently been refined[11] to a value of 3.876. The Th/U of the terrestrial upper mantle, as inferred from analyses of MORBs, is notably lower than this value; two global studies of MORB yield a mean Th/U of ~3.1 (refs 12, 13). The low Th/U of the upper mantle is explained by addition of significant recycled U from the surface and can be reconciled with a surprisingly high time-integrated Th/U (ref. 14), as gauged from $^{208}Pb/^{206}Pb$ ratios, if the U recycling commenced in the latter half of Earth history[2–8]. This makes good geological sense, as before the Great Oxidation Event (GOE) ~2.4 Gyr ago (see, for example, ref. 15) a reduced atmosphere inhibited the surface mobility of U and prevented U recycling.

Here we test and extend this model of global U cycling using isotopic measurements of U to complement the inferences from elemental Th/U. Recent work[16,17] has shown that surface processes induce U isotopic variations (~1‰) that are significantly greater than the typical analytical precision (~0.05‰). Natural variations in $^{238}U/^{235}U$ are chiefly linked to the reduction of U(VI) to U(IV), and the magnitudes of such fractionations are inversely proportional to temperature[18,19]. So whereas U isotopic ratios can be perturbed at the surface, the high temperatures and dominance of tetravalent U in the mantle inhibit significant isotopic fractionations at depth. Any 'exotic' $^{238}U/^{235}U$ signatures, produced by low-temperature fractionation and transported into the mantle, should therefore provide a robust tracer of surface-processed U.

To explore this possibility, we have characterized, to high precision, the $\delta^{238}U$ (the parts per thousand difference in $^{238}U/^{235}U$ relative to a reference solution standard, CRM 145) of a range of samples including meteorites, mantle-derived basalts, and the inputs and outputs of an archetypal subduction zone. A summary of our results is plotted in Fig. 1 and reported in Table 1. Measurement precision varied with sample size, but typically the magnitude of the error in $\delta^{238}U$ was less than ±0.03‰ (2 s.e.). For most samples, the resolution of natural variability was limited by our long-term reproducibility. This was gauged from repeat measurements of the geological standard BHVO-2, which yielded $\delta^{238}U = -0.314‰ \pm 0.028‰$ (2 s.d. on 21 replicates). We additionally obtained $^{234}U/^{238}U$ measurements, which provide a valuable monitor of recent U disturbance. All key samples gave values within error (±3‰) of secular equilibrium for ($^{234}U/^{238}U$), the $^{234}U/^{238}U$ activity ratio. Further details of our analytical procedures and values for a wider range of standards measured are provided in Methods.

Primitive, chondritic meteorites are typically used as a reference for bulk planetary compositions, and so we analysed several ordinary chondrites to try to define a reference 'bulk Earth' $\delta^{238}U$. The very low U contents of chondrites make high-precision measurements especially challenging, so we further analysed two eucrites. These higher-[U] samples should still provide a useful planetary datum given the incompatible, lithophile and refractory nature of U. Our meteorite analyses have $\delta^{238}U$ values that range from −0.44‰ to −0.30‰, overlapping with two existing, lower precision determinations of chondritic $\delta^{238}U$ ($-0.42 \pm 0.09‰$ (ref. 20) and $-0.37 \pm 0.09‰$ (ref. 21)). The variability in $\delta^{238}U$ of our meteorite analyses, however, is greater than the measurement precision and probably reflects recent disturbance of some of our samples (Methods). Thus, we propose a planetary estimate based on the weighted average of the two unaltered samples, with ($^{234}U/^{238}U$) within error of unity. This yields $\delta^{238}U = -0.306 \pm 0.026‰$.

We wish to compare the $\delta^{238}U$ of the terrestrial mantle with this new meteoritic datum, inferred to represent bulk Earth. To this end, we have analysed a wide range of basalts (Methods), which effectively sample the mantle for an incompatible element such as U. Whereas the shallow convecting mantle is probed by MORBs, OIBs are widely assumed to be generated from hot, upwelling plumes (possibly containing components from recycled plates) that provide a window into the deeper mantle. We have analysed fresh MORB glass from all three major oceanic basins and OIBs that cover a large portion of mantle heterogeneity as gauged from radiogenic isotopic compositions. It is clear from Fig. 1 and Table 1 that MORBs and OIBs have different mean $\delta^{238}U$. OIBs with a wide range of Th/U have $\delta^{238}U$ within the error of the bulk Earth, whereas MORBs have significantly higher $\delta^{238}U$ at lower Th/U. The strikingly superchondritic $\delta^{238}U$ we observe in MORBs would strongly support the scenario of widespread pollution of the upper mantle with

[1]Bristol Isotope Group, School of Earth Sciences, University of Bristol, Bristol BS8 1RJ, UK. [2]Institute of Geochemistry and Petrology, Department of Earth Sciences, ETH Zürich, 8092 Zürich, Switzerland. [3]Department of Geology and Geophysics, University of Wyoming, Laramie, Wyoming 82071-2000, USA. [4]Department of Earth Sciences, Durham University, Durham DH1 3LE, UK. [5]Graduate School of Oceanography, University of Rhode Island, Narragansett, Rhode Island 02882-1197, USA.

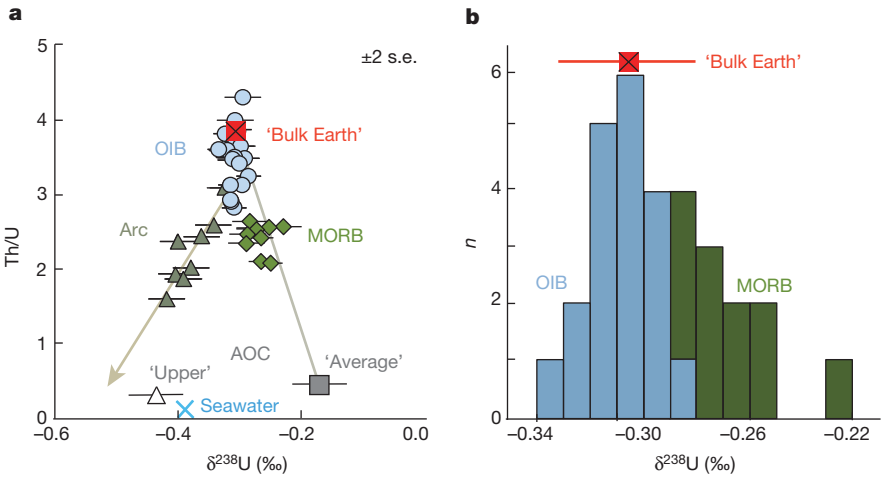

Figure 1 | Uranium isotopic compositions ($\delta^{238}U$) versus Th/U ratios for mantle-derived basalts and altered oceanic crust. **a**, OIBs (circles) have $\delta^{238}U$ similar to the bulk Earth (crossed square), whereas the higher $\delta^{238}U$ and lower Th/U of MORBs (diamonds) imply a mixture (shown as a grey line) between bulk Earth and average modern altered oceanic crust (AOC; square, showing the ODP Site 801 supercomposite). Mariana arc basalts (triangles) show positive covariation of Th/U and $\delta^{238}U$, reflecting the mixing of two components: a sedimentary source, with high Th/U and $\delta^{238}U$; and a source with low Th/U and low $\delta^{238}U$ similar to the upper section of the AOC (open triangle, showing the 0–110 m ODP Site 801 composite). The brown arrow shows the best fit of the Mariana arc data pointing towards the inferred fluid component from the AOC. **b**, Histogram highlighting the distinctively heavy U isotope composition of MORBs relative to the bulk Earth and most OIBs.

surface U, if recycled U were isotopically heavy. Thus, we examine the U isotopic composition of the subducting plate.

Although variations in $\delta^{238}U$ in the sedimentary environment are now established, appropriate measurements to characterize subducted materials are unavailable. We principally focus on determining the isotopic composition of U added by submarine alteration to the igneous oceanic crust, which is the key flux in accounting for the low Th/U of MORBs[6,8]. Comprehensive studies of cores obtained from deep drilling through oceanic crust[8,22,23] (see also the review in ref. 24) demonstrate that heterogeneous addition of U has occurred throughout the upper ~500 m of the mafic AOC. Subduction of this 'excess' U is sufficient to lower the Th/U of the upper mantle to 2.5 in ~2 Gyr (ref. 6).

We have analysed 'composite' samples from ODP Site 801, which penetrates 420 m into ~170 Myr-old Pacific mafic crust[25]. The composites are mixtures of the different lithologies and alteration styles present, blended as powders in representative proportions. This is an efficient means of obtaining a reliable average composition of the heterogeneously altered mafic crust[22,25]. The $\delta^{238}U$ of the composites varies from −0.45‰ in the uppermost part (0–110 m) to higher values (−0.15‰ to +0.16‰) in the deeper parts (110–420 m) (Table 1). This variability probably reflects a change from oxic incorporation of U near the surface[26] to (partial) reductive U roll-front-type sequestration[27], in keeping with a generally observed change in alteration style[8,25]. The 'supercomposite' from ODP Site 801, representing a weighted average of the full 420 m upper crustal section, has $\delta^{238}U = -0.17$‰ and $[U] = 0.39\ \mu g\ g^{-1}$, which is five times higher than the unaltered basalts[8]. This superchondritic value for the average $\delta^{238}U$ reflects the dominance of reductive addition of U(IV) to the upper oceanic crust as a whole (Methods). Interestingly, MORB compositions lie close to a simplistic mixing line between this average altered crustal composition and the bulk Earth reference (Fig. 1).

Table 1 | Summary of $\delta^{238}U$ for sample groups

Sample type	$\delta^{238}U \pm 2$ s.e	Th/U	*N*
Unaltered meteorites (bulk Earth)	−0.306 ± 0.026	3.84	2
OIBs	−0.308 ± 0.005	3.48	19
MORBs	−0.268 ± 0.011	2.44	11
Mafic AOC			
Average	−0.170 ± 0.026	0.44	1
0–110 m	−0.436 ± 0.042	0.30	3
110–220 m	+0.164 ± 0.086	0.45	3
220–420 m	−0.145 ± 0.045	0.44	3
Mariana arc lavas			
Guguan (fluid rich)	−0.405 ± 0.023	1.73	2
Uracas (sediment rich)	−0.333 ± 0.016	2.84	2
Average Mariana sediments	−0.354 ± 0.039	—	7
Seawater (open ocean)	−0.390 ± 0.006	—	3

A full table with individual data is presented in Supplementary Table 1.

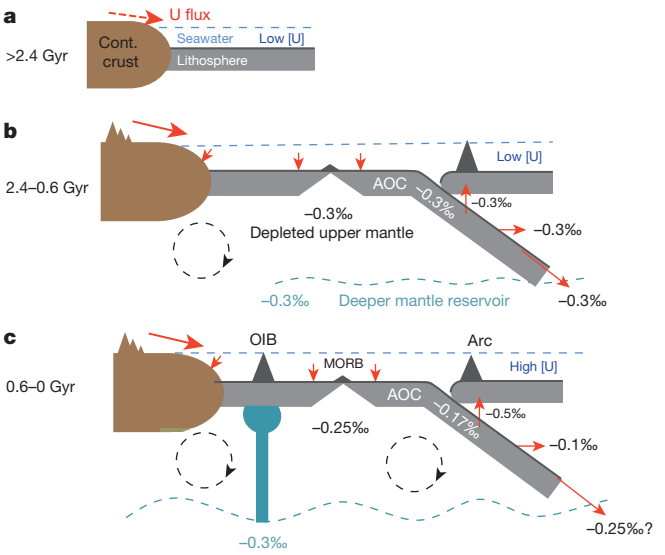

Figure 2 | Cartoon of the terrestrial U isotope cycle over the history of Earth. **a**, Prior to the GOE ~2.4 Gyr ago, low atmospheric oxygen levels limited U mobility on the surface. **b**, The GOE would have heralded an enhanced U weathering flux to the oceans. Quantitative release of U during weathering would yield a U flux to the oceans with $\delta^{238}U \approx -0.3$‰, and quantitative extraction of U into the dominant reducing sinks from the ocean, including AOC, would also give $\delta^{238}U \approx -0.3$‰ for any recycled U delivered to the mantle. **c**, During the past 600 Myr U has been isotopically fractionated during partial, reductive uptake of U into the AOC from the now largely oxic oceans. This fractionated U in the subducted AOC U flux is released at different depths; initially the isotopically light U in the uppermost crust is lost to arc magmatism, and the heavy U from the deeper crust is released beyond the arc front into the convecting upper mantle. The residual, deep-subducted crust has a U isotopic composition similar to unaltered MORB.

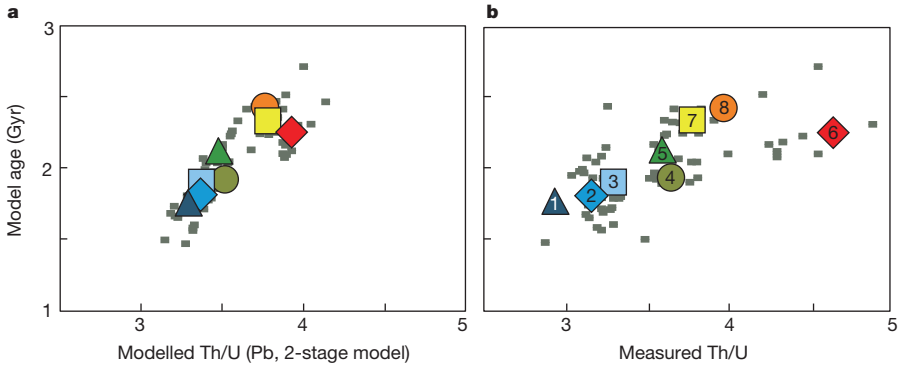

Figure 3 | Pb model ages versus Th/U in OIB mantle sources. Two-stage Pb model ages (^{207}Pb–^{206}Pb ages[10]) versus time-integrated Th/U, using measured ^{208}Pb–^{206}Pb and model source ages (**a**) and measured Th/U for the same suite of OIB samples (**b**): Hawaii (1), Iceland (2), Azores I (3), La Palma (4), French Polynesia (5), Samoa (6), Azores II (7) and Réunion (8) (Methods). Despite potential recent disturbance of the measured Th/U in OIB samples, both plots document a similar relationship of decreasing Th/U with decreasing Pb model ages. These increasingly subchondritic Th/U ratios are consistent with progressive U addition to the mantle from subduction since the GOE ~2.4 Gyr ago.

Finally, we assess the consequences of subduction for the U isotope composition of recycled crust, using the Mariana arc as a well-understood example. During subduction, material is lost from the downgoing plate and is incorporated into magmas erupted at island arcs. The Mariana arc lavas show evidence for two slab-derived components; a melt from the sedimentary section and a 'fluid' from the mafic oceanic crust[28]. A regression line through the array of Marianas lavas in Fig. 1 should point towards the sediment component at high Th/U and the fluid component at low Th/U. The average δ^{238}U of sediments subducting beneath the Mariana (−0.35‰ ± 0.04‰; Table 1) is compatible with the compositions of the lavas with high Th/U, and an extension of the array of Mariana arc lavas to low Th/U indicates that the fluid derived from the mafic oceanic crust has a low δ^{238}U. Such an isotopically light composition can be explained if either the U is preferentially lost from the uppermost altered mafic crust (Fig. 1), or U isotopes are fractionated during (partial) loss from the plate. In either case, the U that is lost to the arc is isotopically lighter than the bulk input to the subduction zone, and so U transported beyond the arc must become even heavier than its initial composition.

Thus, we are confident that modern surface cycling of U results in a substantial flux of isotopically heavy U into the mantle. This observation provides a ready explanation for the superchondritic δ^{238}U of MORBs. The isotopically heavy U must be carried in the altered, mafic crust beyond the zone of arc magmatism, but subsequently lost to the upper mantle (Fig. 2). Transport of U in an accessory mineral such as allanite[29] is a possible means of effecting this outcome.

Like MORBs, many OIBs have significantly subchondritic Th/U, indicative of the addition of recycled U to their sources. Yet all OIBs have δ^{238}U within the error of the bulk Earth value, which is inconsistent with the modern U cycle. We noted above, however, that the high δ^{238}U characteristic of average recent oceanic crust is the result of partial reduction of U-rich, oxidized seawater as it percolates through the submarine volcanic edifice. This scenario has been possible only in the last ~600 Myr, since the second rise in oxygen in the late Proterozoic eon and the establishment of fully oxic oceans (see, for example, ref. 15). Between 600 Myr ago and the initial rise of oxygen ~2.4 Gyr ago, U was mobile during surface weathering but was rapidly scavenged from the reduced oceans[15]. Quantitative removal of riverine U supplied to the oceans would result in a flux of U to the sea floor that was isotopically unfractionated (Fig. 2 and Methods). The implications of this conceptual model are that OIB sources formed from recycled oceanic crust between 2.4 and 0.6 Gyr ago should have increasingly subchondritic Th/U, but chondritic δ^{238}U. Furthermore, any OIB source formed earlier than 2.4 Gyr ago should have both chondritic Th/U and chondritic δ^{238}U.

We have further investigated this idea using Pb model ages of several OIB suites. Their Pb model ages are calculated using a two-stage model, similar to that of ref. 10 (Methods). As in ref. 10, we find that OIBs have a range of source model ages. Notably, these ages correlate with the Th/U of the samples (Fig. 3), in the manner discussed above. We show two plots in Fig. 3: one with time-integrated Th/U as determined from Pb isotopes (Fig. 3a), and the other with measured Th/U (Fig. 3b). Not unsurprisingly, the data using time-integrated Th/U form a tighter array, because any recent Th/U fractionations from source composition during melting and melt migration to the surface are removed (Methods). However, both plots independently document a similar relationship, with Th/U becoming increasingly subchondritic in OIB sources younger than ~2.4 Gyr.

The remarkable implication of the ideas presented above is that the two-stage rise in atmospheric oxygen, reconstructed from observations on the Earth's surface, is reflected in the Th–U–Pb systematics of mantle-derived basalts. The coherence of our observations with those anticipated from a first-order model of U recycling also lends credence to the significance of Pb model ages of OIB sources[10]. The range of OIB model ages therefore places valuable constraints on the maximum and minimum incubation times of an OIB reservoir, which may be the longest and shortest residence times of subducted slabs at the base of the mantle before they become sufficiently buoyant to return to the surface. Furthermore, our inference that isotopically heavy U has been introduced into the mantle over only the last 600 Myr yields a maximum timescale for its effective stirring into the MORB source. This value is reassuringly consistent with an estimate based on a markedly different approach using Pb isotopes[30].

Online Content Methods, along with any additional Extended Data display items and Source Data, are available in the online version of the paper; references unique to these sections appear only in the online paper.

Received 11 July; accepted 4 November 2014.

1. Albarède, F. & Michard, A. Transfer of continental Mg, S, O and U to the mantle through hydrothermal alteration of the oceanic crust. *Chem. Geol.* **57,** 1–15 (1986).
2. Zartman, R. E. & Haines, S. M. The plumbotectonic model for Pb isotopic systematics among major terrestrial reservoirs: a case for bi-directional transport. *Geochim. Cosmochim. Acta* **52,** 1327–1339 (1988).
3. McCulloch, M. T. The role of subducted slabs in an evolving earth. *Earth Planet. Sci. Lett.* **115,** 89–100 (1993).
4. Kramers, J. D. & Tolstikhin, I. N. Two terrestrial lead isotope paradoxes, forward transport modelling, core formation and the history of the continental crust. *Chem. Geol.* **139,** 75–110 (1997).
5. Collerson, K. D. & Kamber, B. S. Evolution of the continents and the atmosphere inferred from Th-U-Nb systematics of the depleted mantle. *Science* **283,** 1519–1522 (1999).
6. Elliott, T., Zindler, A. & Bourdon, B. Exploring the kappa conundrum: the role of recycling in the lead isotope evolution of the mantle. *Earth Planet. Sci. Lett.* **169,** 129–145 (1999).
7. Zartman, R. E. & Richardson, S. H. Evidence from kimberlitic zircon for a decreasing mantle Th/U since the Archean. *Chem. Geol.* **220,** 263–283 (2005).

8. Kelley, K. A., Plank, T., Farr, L., Ludden, J. & Staudigel, H. Subduction cycling of U, Th, and Pb. *Earth Planet. Sci. Lett.* **234,** 369–383 (2005).
9. White, W. M. & Hofmann, A. W. Sr and Nd isotope geochemistry of oceanic basalts and mantle evolution. *Nature* **296,** 821–825 (1982).
10. Chase, C. G. Oceanic island Pb: two-stage histories and mantle evolution. *Earth Planet. Sci. Lett.* **52,** 277–284 (1981).
11. Blichert-Toft, J., Zanda, B., Ebel, D. S. & Albarède, F. The Solar System primordial lead. *Earth Planet. Sci. Lett.* **300,** 152–163 (2010).
12. Gale, A., Dalton, C. A., Langmuir, C. H., Su, Y. & Schilling, J. G. The mean composition of ocean ridge basalts. *Geochem. Geophys. Geosyst.* **14,** 489–518 (2013).
13. Jenner, F. E. & O'Neill, H. S. C. Analysis of 60 elements in 616 ocean floor basaltic glasses. *Geochem. Geophys. Geosyst.* **13,** 1–11 (2012).
14. Galer, S. J. G. & O'Nions, K. Residence time of thorium, uranium and lead in the mantle with implications for mantle convection. *Nature* **316,** 778–782 (1985).
15. Lyons, T. W., Reinhard, C. T. & Planavsky, N. J. The rise of oxygen in Earth's early ocean and atmosphere. *Nature* **506,** 307–315 (2014).
16. Stirling, C. H., Andersen, M. B., Potter, E.-K. & Halliday, A. N. Low temperature isotope fractionation of uranium. *Earth Planet. Sci. Lett.* **264,** 208–225 (2007).
17. Weyer, S. *et al.* Natural fractionation of $^{238}U/^{235}U$. *Geochim. Cosmochim. Acta* **72,** 345–359 (2008).
18. Fujii, Y., Nomura, M., Onitsuka, H. & Takeda, K. Anomalous isotope fractionation in uranium enrichment processes. *J. Nucl. Sci. Technol.* **26,** 1061–1064 (1989).
19. Bigeleisen, J. Temperature dependence of the isotope chemistry of the heavy elements. *Proc. Natl Acad. Sci. USA* **93,** 9393–9396 (1996).
20. Connelly, J. N. *et al.* The absolute chronology and thermal processing of solids in the solar protoplanetary disk. *Science* **338,** 651–655 (2012).
21. Goldmann, A., Brennecka, G., Noordmann, J., Weyer, S. & Wadhwa, M. The $^{238}U/^{235}U$ of the Earth and the Solar System. *Geochim. Cosmochim. Acta* **148,** 145–158 (2015).
22. Staudigel, H., Davies, G. R., Hart, S. R., Marchant, K. M. & Smith, B. M. Large scale isotopic Sr, Nd and O isotopic anatomy of altered oceanic crust: DSDP/ODP sites 417/418. *Earth Planet. Sci. Lett.* **130,** 169–185 (1995).
23. Bach, W., Peucker-Ehrenbrink, B., Hart, S. R. & Blusztajn, J. S. Geochemistry of hydrothermally altered oceanic crust: DSDP/ODP Hole 504B: implications for seawater-crust exchange budgets and Sr- and Pb-isotopic evolution of the mantle. *Geochem. Geophys. Geosyst.* **4,** 8904 (2003).
24. Dunk, R. M., Mills, R. A. & Jenkins, W. J. A reevaluation of the oceanic uranium budget for the Holocene. *Chem. Geol.* **190,** 45–67 (2002).
25. Kelley, K. A., Plank, T., Ludden, J. & Staudigel, H. Composition of altered oceanic crust at ODP Sites 801 and 1149. *Geochem. Geophys. Geosyst.* **4,** 8910 (2003).
26. Brennecka, G. A., Wasylenki, L. E., Bargar, J. R., Weyer, S. & Anbar, A. D. Uranium isotope fractionation during adsorption to Mn-oxyhydroxides. *Environ. Sci. Technol.* **45,** 1370–1375 (2011).
27. Bopp, C. J. IV, Lundstrom, C. C., Johnson, T. M. & Glessner, J. J. Variations in $^{238}U/^{235}U$ in uranium ore deposits: isotopic signatures of the U reduction process? *Geology* **37,** 611–614 (2009).
28. Elliott, T., Plank, T., Zindler, A., White, W. & Bourdon, B. Element transport from slab to volcanic front at the Mariana arc. *J. Geophys. Res.* **102,** 14991–15019 (1997).
29. Hermann, J. Allanite: thorium and light rare earth element carrier in subducted crust. *Chem. Geol.* **192,** 289–306 (2002).
30. Rudge, J. F. Mantle pseudo-isochrons revisited. *Earth Planet. Sci. Lett.* **249,** 494–513 (2006).

Supplementary Information is available in the online version of the paper.

Acknowledgements Financial support for this research was provided by NERC grant NE/H023933/1. We thank the Natural History Museum, London, and M. Anand for providing meteorite samples. H. Staudigel and T. Plank were instrumental in producing and curating AOC composite samples. We are grateful to C. Taylor for careful picking of MORB glasses, E. Melekhova for preparing the quenched glass, D. Vance for comments and C. Coath for maintenance of the mass spectrometers.

Author Contributions Analytical set-up was done by M.B.A. Sample preparation and analyses were carried out by M.B.A. and H.F. MORB samples and AOC composites were provided by K.W.W.S., Y.N. and K.A.K. All authors contributed with discussions. T.E. carried out the Pb modelling. T.E. and M.B.A. prepared the manuscript.

Author Information Data can be found in the EarthChem portal (http://www.iedadata.org). The nine-digit IGNS numbers for the sample set starts with 'IEMBA'. Reprints and permissions information is available at www.nature.com/reprints. The authors declare no competing financial interests. Readers are welcome to comment on the online version of the paper. Correspondence and requests for materials should be addressed to M.B.A. (morten.andersen@erdw.ethz.ch).

METHODS

Sample preparation. With two main exceptions, existing powders of samples were used for this study. Preparation techniques for these powders are documented in the associated studies. Powdered samples of bulk meteorites were prepared at the University of Bristol for this study, from chips carefully picked under the microscope to be free from alteration, fusion crust or signs of saw-blade marks. Likewise, all MORB samples were prepared afresh by picking millimetre-sized fragments of glass without signs of alteration, surface coatings or devitrification.

Given the low U concentrations of MORB, the consequences of possible secondary U addition by absorption to marine Fe–Mn oxyhydroxide coatings is a concern. Although careful hand-picking should address this problem, we further processed the picked glass, using a mildly reductive procedure based on methods for dissolving Fe–Mn coatings in marine sediments, using a mixture of 0.05 N hydroxylamine hydrochloride, 15% acetic acid and 0.03 N Na-EDTA at pH ~4 (ref. 31). Similar approaches have been used in preparing MORB glasses for U-series analysis[32–34]. Each sample was leached three consecutive times by adding 12 ml of the leaching solution to the bulk samples in pre-cleaned centrifuge tubes, and placing these in a vortex shaker for 24 h at room temperature (~20 °C). Samples were thoroughly rinsed in 18 MΩ cm water following each leaching step.

The elemental concentrations of each leaching solution were determined using the Element 2 ICP-MS of the Bristol Isotope Group, using already established methods[35]. Potential contaminant U removed in each leach fraction was monitored using the total U concentration and the ratios of U to immobile elements Th, Sc, Ti and Zr (Supplementary Table 2). For most samples, the first leach released U in higher proportions than the immobile elements; however, at the end the three leaching steps the ratios of U to the refractory elements approached the ratios measured in the total bulk (residual) MORB sample after full dissolution. This suggests that any minor, absorbed U was effectively leached away. The U removed during reductive leaching represented only 1% to 4% of the total U that remained in the bulk residue. All MORB samples have ($^{234}U/^{238}U$) within a few per mil of secular equilibrium, except D18-1, which had a ($^{234}U/^{238}U$) ~14‰ above secular equilibrium, suggesting that some U contaminant was still present after the reductive leaching. The elevated ($^{234}U/^{238}U$) of seawater (1.146) suggests that this contamination is marine derived. Despite the minor residual U contamination, we have chosen to leave it in our data set, but note its value is not as robust as the other measurements (see below for further discussion).

In addition to the natural samples, a basalt powder was made into a glass and leached to assess whether the reductive leaching caused any U isotope fractionation in the residual glass. Given the small total amounts of U removed during leaching and that the final leaching solutions appeared to have removed material with bulk glass composition (Supplementary Table 2), it seemed unlikely that leaching would bias the U isotopic composition of the residue; but for completeness we tested this. A basalt powder was melted in a platinum crucible and subsequently quenched by dropping the platinum crucible into a bath of 18 MΩ cm water at room temperature. Given the low ages of the MORB glasses in this study, they have experienced little U-series α-recoil damage and can therefore be directly compared with the leaching of the artificial quenched glass. Measurements of the quenched glass gave identical $\delta^{238}U$ before and after the reductive leaching step (−0.23‰ ± 0.03‰ versus −0.24‰ ± 0.03‰) and identical ($^{234}U/^{238}U$) (0.995 ± 0.003 and 0.999 ± 0.002), showing that the leaching process does not fractionate the U isotopes of fresh glass.

Sample dissolution, spiking and column chemistry. Sample sizes up to ~1.5 g were dissolved in a single beaker. For larger samples (for example chondrites and MORB) several splits of the same sample were dissolved separately and then all aliquots were combined after full dissolution. Terrestrial silicates were dissolved in a mixture of concentrated $HF/HNO_3/HClO_4$ acid, fluxed on a hotplate for 24 h and dried by stepwise-increasing the temperature from 120 °C to 200 °C. Samples were then fluxed twice in ~6 N HCl (~15 ml per gram of sample) on a hotplate (120 °C) and dried down in between. Samples were redissolved in 7 N HNO_3 and then diluted down to 2 N HNO_3 for TRU Resin column chemistry. Both the eucrites (~1 g) and the ordinary chondrites (~4 g in three aliquots) were initially dissolved in a similar way to larger terrestrial silicate samples. However, after the 7 N HNO_3 step the dissolution was incomplete and a residue of dark residue remained. These residues were isolated from the remaining dissolved sample and refluxed in a mixture of 3 ml concentrated HNO_3 and 1 ml concentrated HCl in a high-pressure, Anton-Paar asher (200 °C and 100 bar pressure, in silica glass vials). This step fully dissolved the residues, which were then remixed with the already dissolved sample aliquots, dried down and redissolved in 7 N HNO_3 before TRU Resin chemistry in 2 N HNO_3.

All samples were spiked with the IRMM-3636 ^{233}U–^{236}U double spike[36] (aiming for $^{236}U/^{235}U$ of ~5), either before dissolution or before column chemistry for samples combined from separately processed aliquots.

The U was separated from all other matrices in a two-step procedure by TRU Resin and UTEVA chemistry. The TRU Resin chemistry was optimized for large sample sizes with ~2 ml resin loaded in polypropylene Bio-Rad columns. Up to ~1 g of sample was loaded on each column. Samples were loaded and matrix eluted using 40 ml 2 N HNO_3, and U was collected in 8 ml 0.3 N HF/0.1 N HCl. Samples were then dried down and fluxed in concentrated HNO_3/H_2O_2 to eliminate any organic material from the resin bleeding into the sample. For large samples that were split over several columns, these were homogenized at the end of this phase and then dried down to be redissolved in 3 N HNO_3 for UTEVA chemistry. The UTEVA chemistry was performed in shrink-fit Teflon columns containing ~0.6 ml of resin. Loading and matrix elution steps used 20 ml of 3 N HNO_3, before elution of Th in 3 ml of 3 N HCl, and collection of the purified U in 8 ml 0.3 N HF/0.1 N HCl. Samples were then dried down, fluxed in concentrated HNO_3/H_2O_2, dried down and redissolved in the requisite amount of 0.2 N HCl for the desired U concentration (100–300 p.p.b.) for MC-ICPMS measurements. Full U recovery (>95%) was obtained using this method with total chemistry blanks of <20 pg for all samples (negligible compared with sample sizes >20 ng).

MC-ICPMS measurement set-up. The U isotope measurements were conducted on a Thermo Finnigan Neptune MC-ICP-MS (serial no. 1002) of the Bristol Isotope Group, running in low mass resolution ($M/\Delta M \approx 500$) and using an Aridus desolvating nebulizer introduction system. Uranium sample sizes of 40–150 ng were consumed during individual analysis. The data were collected in static mode in a similar fashion to that described in ref. 37. All cups were connected to feedback amplifiers with 10^{11} Ω resistors, except for the ^{238}U cup, which was connected to a feedback amplifier with a 10^{10} Ω resistor to accommodate a larger ion beam. Uranium tailing and hydride formation were monitored as described in ref. 37. Both the 237.05/^{238}U abundance sensitivity and the hydride and high-side tailing formation at 1 a.m.u. (measured as 239.05/^{238}U) were $(2–3) \times 10^{-6}$, and remained stable during each measurement session. The low-mass side-tailing contributions to ^{233}U, ^{234}U, ^{235}U and ^{236}U were estimated, and corrected for, from interpolation of a linear–log fit to mass versus tailing intensity, as used in ref. 38. Furthermore, corrections for $^{232}ThH^+$ and 1 a.m.u. high-mass tailing on ^{233}U were made to measurement, assuming similar behaviour for Th and U. These were of minimal importance, however, owing to the good separation of U from Th during the UTEVA chemistry ($^{232}Th/^{233}U < 1$).

Measurements were conducted using typical ion beam intensities of ~1 nA for ^{238}U, ~7 pA for ^{235}U, ~40 pA for ^{236}U and ^{233}U, and ~0.05 pA for ^{234}U, integrated over a period of 80 × 4 s. Washout and on-peak blank measurements were similar to those described in ref. 37. On-peak U blank intensity never exceeded 10 p.p.m. of the total ^{238}U beam of the sample and was generally <2 p.p.m.

The Neptune was equipped with a large plasma interface pump (turbo-booster) offering enhanced transmission efficiency when combined with 'jet+X cones', as opposed to 'standard+X cones'. The data obtained are identical for both set-ups (Supplementary Tables 3 and 4). General U transmission efficiencies were ~1.5% for standard+X cones and ~3% for jet+X cones.

After tailing and hydride corrections, the measured $^{233}U/^{236}U$ ratio was used for mass bias correction, using the exponential mass fractionation law[39]. To obtain $^{234}U/^{238}U$ and $^{235}U/^{238}U$ ratios, the minute ^{238}U, ^{235}U and ^{234}U contributions from the IRMM-3636 spike were subtracted. Based on a calibration using CRM-145 (Supplementary Table 3), the U isotope ratios used for the Bristol IRMM-3636 were $^{236}U/^{233}U = 0.98130$, $^{236}U/^{238}U = 4{,}259$, $^{236}U/^{235}U = 21{,}988$ and $^{236}U/^{234}U = 2{,}770$. These ratios are identical to the certified ratios from IRMM-3636[36] for $^{236}U/^{233}U$ (0.98130 ± 0.00015), $^{236}U/^{238}U$ (4,259 ± 7) and $^{236}U/^{235}U$ (21988 ± 36), but diverge slightly for $^{236}U/^{234}U$ (2732 ± 4). Measurements of all unknown samples were bracketed individually and normalized to CRM-145 standard measurements, spiked with IRMM-3636, in a similar fashion to the unknowns.

Measurement performance, reproducibility and accuracy. For each measurement sequence, the mean of the absolute $^{238}U/^{235}U$ of the CRM-145 standard used was typically within ±50 p.p.m. of the value (137.832) reported for the NBL 112a standard[38], and the $^{234}U/^{238}U$ ratios were within ±2‰ of published ratios for the CRM-145 standard[37]. The ($^{234}U/^{238}U$) activity ratios were calculated using the half-lives in ref. 40. All samples in this study were normalized to the CRM-145 standard, such that any deviations relative to the absolute ratio of the CRM-145 standard, potentially related to a non-exponential component of instrumental mass fractionation, are corrected.

Given the use of mixed feedback amplifier resistors with different response times, internal error estimates may give a misleading impression of true precision (see, for example, ref. 41). Thus, to test the full external reproducibilities for individual unknown samples, a total of eight splits of BHVO-2 were individually processed (dissolution, spiking and chemistry) and measured during different analytical sessions (with different set-ups; see Supplementary Table 4). The external reproducibility of $\delta^{238}U$ for BHVO-2 was ±28 p.p.m. (2 s.d.) and a similar or better external reproducibility was obtained for the basalt LP 45 E (a historic basanite from La Palma), the in-house CZ-1 uraninite and three open-ocean seawater samples (Extended Data Fig. 1). Other samples measured in duplicate agreed within their 2 s.e. estimates

(Supplementary Table 4). The reproducibilities of $^{234}U/^{238}U$ were limited by the low ^{234}U intensities (<0.2 pA), but were ±3‰ or better for the standards.

Potential artefacts in the measured $\delta^{238}U$ from different U/matrix ratios are unlikely given that ordinary chondrites (low U/matrix ratio) and OIB (high U/matrix ratio) both have lower $\delta^{238}U$ compared with MORB (intermediate U/matrix ratio). Furthermore, consistent results are obtained when comparing the standards measured in this study and other studies using comparable normalizing standards (NBL 112a[17], SRM-950a[21] and CRM-145[16]). The measured uraninite CZ-1 standard ($\delta^{238}U = -0.053‰ \pm 0.029‰$) is within error of the value reported in ref. 16 ($-0.10‰ \pm 0.07‰$). Similarly, the BHVO-2 measurements in this study ($\delta^{238}U = -0.314‰ \pm 0.028‰$) compare well with measurements in ref. 21 ($-0.32‰ \pm 0.07‰$). Finally, our open-ocean seawater measurements ($\delta^{238}U = -0.390‰ \pm 0.018‰$) agree well with open-ocean seawater measurements in ref. 17 ($-0.41‰ \pm 0.03‰$).

Uranium in extraterrestrial material and a bulk Earth $\delta^{238}U$. Previous work has shown large variability in the $\delta^{238}U$ of extraterrestrial material[20,21,42–46]. Thus, even if it exists, estimating a uniform chondritic $\delta^{238}U$ composition is challenging. Some of the observed $\delta^{238}U$ heterogeneity has been attributed to variable addition of ^{235}U from the decay of, now extinct, ^{247}Cm (ref. 45). However, meteorites also show relative depletions in ^{235}U, indicating that other processes may have a role[20,21,42,46] (for example nucleosynthetic anomalies or planetary formation processes). An additional concern is terrestrial perturbation of U, which may be indicated from the physical preservation and anomalous chemical composition. Specifically for U, Th/U departing from the recently defined meteoritic reference[11] and ($^{234}U/^{238}U$) activity ratios out of secular equilibrium may testify to planetary body processes[47] or terrestrial perturbation.

Owing to the generally low U abundance in meteorites, it is necessary to obtain large chondrite samples (~5–10 g) to allow high-precision $\delta^{238}U$ measurements, which can run counter to museum loan policies. Thus, we initially honed our technique on three large desert meteorite 'finds' (M2, M12 and M15), provided by M. Anand from the Open University. These had previously been studied petrographically and characterized at the University of Bristol. We had prepared several hundred grams of powder from the interiors of these ordinary chondrites. As finds, however, these samples were potentially perturbed by terrestrial weathering. We subsequently obtained large (~25 g) samples of two 'falls' (Zag and Saratov) from the Meteorite Market (http://www.meteoritemarket.com/). All these samples are ordinary chondrites, which are not only more readily available than carbonaceous chondrites, but are isotopically more similar to the Earth (see, for example, refs 48, 49).

We supplemented our ordinary chondrite measurements with analyses of two eucrites, Juvinas and Stannern, kindly provided by the Natural History Museum, London. Eucrites have higher U contents and so require smaller sample sizes (~1 g) for high-precision analyses. Although differentiated meteorites, the isotope ratio of a highly incompatible element such as U should be minimally affected during crust formation, and so we believe that these samples still provide a valuable planetary reference. Notably, eucrites generally have chondritic Th/U ratios[50–52], indicating an absence of elemental fractionation during their formation. The eucrite samples we analysed were falls, and so are probably less prone to terrestrial weathering than the finds.

Of the ordinary chondrites, two gave identical, but relatively low, $\delta^{238}U$ ratios (M15 ($-0.439‰ \pm 0.030‰$) and Saratov ($-0.442‰ \pm 0.050‰$)), whereas the three others were all within error but were ~100 p.p.m. higher (M2 ($-0.322‰ \pm 0.030‰$), M12 ($-0.326‰ \pm 0.022‰$) and Zag ($-0.301‰ \pm 0.050‰$)). The eucrites also differed in their $\delta^{238}U$ (Juvinas ($-0.312‰ \pm 0.030‰$) and Stannern ($-0.369‰ \pm 0.030‰$)), but with Juvinas overlapping with the compositions of the heaviest ordinary chondrites (Extended Data Fig. 2).

The three ordinary chondrite desert finds have elevated ($^{234}U/^{238}U$) ratios (1 to 12% ^{234}U excess) suggesting oxidative weathering during their time at the Earth's surface, with oxidation of Fe potentially promoting mineral surfaces for U sorption, with a positive correlation between U concentration and ($^{234}U/^{238}U$) ratios (Extended Data Fig. 2). Furthermore, Saratov also had ~1% elevated ($^{234}U/^{238}U$), whereas Stannern was ~1% depleted in ($^{234}U/^{238}U$) relative to secular equilibrium. Only the ordinary chondrite Zag and eucrite Juvinas were at secular equilibrium for ($^{234}U/^{238}U$). The independent constraints provided by ($^{234}U/^{238}U$) show that only Juvinas and Zag can be considered pristine and, notably, their $\delta^{238}U$ values are within error of each other (Extended Data Fig. 2).

Perturbation of U in the meteorite samples is also indicated by their Th/U ratios relative to the planetary reference value[11] of 3.876 ± 0.016. The ordinary chondrites with the lowest $\delta^{238}U$ have the highest [U] and lowest Th/U, further suggestive of U addition. Three samples (Juvinas, Zag and M2) have Th/U within error of the reference value, and all have $\delta^{238}U$ values within error of each other (Extended Data Fig. 2). However, given the minor ($^{234}U/^{238}U$) excess in M2, we do not include this in our best estimate of the bulk Earth value, $\delta^{238}U = -0.306‰ \pm 0.026‰$, provided by the weighted average and weighted 2 s.e. of Juvinas and Zag. Despite demonstrable open-system behaviour of U, the mean of all meteorite samples gives a $\delta^{238}U$ of $-0.36‰ \pm 0.04‰$ (±2 s.e.m.), which is within error of the weighted estimate from pristine samples (Extended Data Fig. 2). Although our best estimate for the bulk Earth from our meteoritic samples is defined by only two samples, and would usefully be substantiated by additional measurements, we believe that the systematics of the altered samples provide important evidence to support the significance of this best estimate. Moreover, in terms of our main observations on terrestrial samples the choice is not critical; for either the mean of all the meteorites or just the pristine ones, the $\delta^{238}U$ of MORB are heavier while the $\delta^{238}U$ of OIBs are unresolved from these meteoritic values.

$\delta^{238}U$ in OIBs. A suite of 19 OIBs from Iceland, Cape Verde, Azores, Canary Islands and Hawaii were measured. Further details on these samples are provided in Supplementary Table 1. We have dominantly used historic samples, collected previously for U-series studies, which have the major advantage of being fresh. Notably, we analysed four non-historic, but still relatively young (~1 Myr) and ostensibly petrographically fresh samples from La Palma, Canary Islands. Two of these samples (LPF 96-39 and CS20) yielded ($^{234}U/^{238}U$) out of equilibrium, warning us against using older samples from possibly more extreme weathering environments elsewhere. Nevertheless, these two samples, showing clear open-system U-series behaviour with ($^{234}U/^{238}U$) ~2% lower than secular equilibrium, are still within error of the other La Palma samples for $\delta^{238}U$, and so we did not exclude these data from our averages. This also indicates that $\delta^{238}U$ is not hugely sensitive to minor perturbations of the U budget.

In terms of traditional radiogenic isotope characterization, the islands we have studied cover high $^{3}He/^{4}He$ (Hawaii, Iceland), HIMU (La Palma, Canaries), EMII (Sao Miguel, Azores) and FOZO (Pico, Azores, and Fogo, Cape Verde) 'flavours' of mantle signature[53–55]. Although La Palma is not as radiogenic in its lead isotope ratios as the classic French Polynesian and St Helena localities, the latter have suffered ~10 Myr of tropical weathering, and so are far from ideal for characterizing primary U isotope ratios. We have not measured any representative samples from EMI-type mantle, but nevertheless cover a large compositional range of OIB.

$\delta^{238}U$ in MORBs. We have measured eleven glassy, axial or near-axial MORB samples from all three major ocean basins: the Indian ($n = 1$), the Atlantic ($n = 3$) and the Pacific ($n = 7$). Further details on these samples are given in Supplementary Table 1 and associated references[56–60]. All picked glasses were leached to remove possible absorbed U on ferro-manganese coating, as discussed earlier. The eleven MORB glasses have Th/U ratios of 2.1 to 2.6 and all have ($^{234}U/^{238}U$) within a few per mil of secular equilibrium, except the already discussed Atlantic Ocean sample D18-1. As for the OIBs with perturbed ($^{234}U/^{238}U$), the $\delta^{238}U$ does not appear strongly affected and D18-1 has $\delta^{238}U = -0.265‰ \pm 0.030‰$, identical to the mean $\delta^{238}U$ of all MORB; we thus did not exclude this data point from our averages. This observation is compatible with a mass balance calculation to account for the observed ($^{234}U/^{238}U$) disequilibrium of D18-1 assuming the contaminant has a U isotope composition similar to seawater. Adding seawater with ($^{234}U/^{238}U$) of 1.146 to MORB at secular equilibrium should result in a change in $\delta^{238}U$ of less than 0.02‰ given a seawater $\delta^{238}U$ of −0.39‰.

$\delta^{238}U$ in island arc volcanics. A suite of nine mafic samples from the Mariana arc front[28] was selected to investigate subduction zone processes (Supplementary Table 1). These well-characterized samples show variable subducted sediment input to their sources, combined with a rather constant flux of 'fluid' from the subducting, mafic oceanic crust[28]. In more detail, it has recently been argued that the sediment component evident in the arc lavas is dominated by the volcaniclastic horizons rather than representing an average of all lithologies, in which pelagic clay has a significant role[28,61]. Samples with small sediment contributions, as marked by high $^{143}Nd/^{144}Nd$ and low Th/Nb, have low Th/U and high ($^{238}U/^{230}Th$), implying a recent, slab-derived U addition to their mantle source. The systematic compositional variations of these lavas allow us to extrapolate to the possible $\delta^{238}U$ of this slab-derived fluid, using a best-fit linear regression line through the data in the Th/U–$\delta^{238}U$ space, as shown in Fig. 1.

$\delta^{238}U$ of subduction zone inputs. Subducted crust can be separated into three principal, chemical components: unaltered oceanic crust, mafic AOC and sediments. Here we analysed sediments and AOC from well-characterized deep-ocean drill holes[8,25,62], ODP Site 801 and ODP Site 802 in the west Pacific, to assess the U budget of subduction-related material. Not only does the former location provide the best opportunity to assess the mean composition of the old AOC (~170 Myr), but because these locations are in front of the Mariana arc, the composition of the overlying sediments are specifically appropriate as the endmember for the Mariana arc lavas.

Typical assemblages for the deeper ocean sediment package that are subducted include volcaniclastics, pelagic clays, cherts, carbonates and Fe–Mn crusts. The U concentrations for these materials are variable in the 0.1–10 μg g^{-1} range. Modern seawater has a U concentration of ~3.2 ng g^{-1} and a homogeneous $\delta^{238}U$ of $-0.390‰ \pm 0.010‰$ (Supplementary Table 1). Biogenic carbonate appears to

incorporate U from seawater without any significant isotope fractionation[63]. The measured deep-sea pelagic clays and volcaniclastics are close to the seawater $\delta^{238}U$ and the bulk Earth value (−0.42‰ to −0.28‰; Supplementary Table 1). Furthermore, the ODP Site 801 composite sample '801SED', meant to reflect an average of the infilling material between the pillow basalts within the basement (comprising chert, hydrothermal deposit, calcite and clay minerals) has a $\delta^{238}U$ similar to seawater. Thus, the Mariana and indeed most subducting sediment packages have an average $\delta^{238}U$ close to the values for modern seawater and bulk Earth.

The most important source of 'U excess' in subduction zones is the AOC. The fluid-induced alteration in oceanic crust can generally be classified into high-temperature (>100 °C) and low-temperature (<100 °C) types.

The high-temperature alteration generally occurs close to the spreading ridge axis and at greater depth in the crust by percolation of hot hydrothermal fluids[64,65]. Any seawater-derived U uptake in these settings is assumed to be quantitative (see, for example, ref. 66); however, the deeper sections of the crust (>1,000 m) affected by high-temperature hydrothermal circulation are generally little altered and have low U concentrations close to typical MORB[65] (for example 0.07 μg g^{-1}). Thus, the high-temperature alteration at greater depth does not appear to add a significant amount of U compared with the shallower, low-temperature alteration[24].

The low-temperature alteration (<100 °C) dominates at ridge-flanks with percolation of less intensely heated seawater[65,67], and the uppermost 500 to 1,000 m of the mafic oceanic crust experiences significant U addition[8,22–25,64] with a mean fivefold-greater U content relative to the unaltered MORBs[8]. The low-temperature alteration is therefore the cause of most uptake of additional U in the subducting plate. Thus, we have focused our attention on characterizing this low-temperature alteration using average, 'composite' samples (see below).

Altered, mafic oceanic crust. For estimating the U concentration and $\delta^{238}U$ budget of altered oceanic crust, we have made high-precision $\delta^{238}U$ analyses of 'composites' from the upper ~500 m of altered extrusive lavas at the well-studied ODP Site 801. This represents a substantial section of the extrusive lavas erupted at a fast spreading centre[68]. Secondary alteration products from hydrothermal seawater flow-through suggest alteration temperatures from 10 to 100 °C, increasing with depth[62]. A typical alteration sequence consists of oxic celadonite formation around alteration veins, followed by Fe-hydroxides and then reducing saponite and pyrite, in a zone moving away from the alteration veins and into the host rock[62]. Carbonate precipitates also occur, which may have formed intermittently through time[8,62]. Uranium enrichments are evident in breccia zones and in relation to redox haloes, with U concentrated at the boundary between oxidized (celadonite-rich) and reduced (saponite/pyrite-rich) zones moving away from the alteration veins, in a roll-front-redox-type U deposition pattern[8,62]. These redox haloes dominate the deeper part of the drilled section[8,62]. In ref. 8 it is estimated that about 50% of the total U excess is hosted in the secondaryily formed carbonates and that the remainder is associated with the redox haloes.

From the main (tholeiitic) ~420 m alteration zone, three suites of composite samples from different depth ranges (0–110 m, 110–220 m, 220–420 m) have been prepared to average the composition of the heterogeneously altered sections in the crust[25]. The composites are physical mixtures of powders in relative proportions of their abundances throughout the particular section of core, and are intended to physically represent the bulk composition of various depth domains within the drilled sequence. For each of the three composite zones three different powder mixtures were prepared: 'FLO' composites represent the least-altered material, 'VCL' the most altered material and 'MORB' composites represent the bulk (mixtures of the FLO and VCL composites)[25]. Furthermore, a 'supercomposite', comprising an integration of the full upper 420 m of core, was made[25]. All the composite samples have low Th/U ratios (0.1–0.6), and high U concentrations of ~0.4 μg g^{-1} (ref. 25). The U concentration of the 801 supercomposite (0.39 μg g^{-1}) is similar to the DSDP 417/418 supercomposite (0.3 μg g^{-1}) and significantly higher than estimated unaltered MORB[69] (0.05 μg g^{-1}).

The $\delta^{238}U$ was measured in the three composite sections (in all three FLO, VCL and MORB powder mixtures), the supercomposite and three individual samples. The $\delta^{238}U$ in the composite samples are variable through the ~420 m sequence: the upper ~110 m averages −0.436‰ ± 0.042‰; the middle ~110 m are significantly heavier, averaging +0.164‰ ± 0.086‰; and the lower ~200 m are in between, averaging −0.145‰ ± 0.045‰ (Supplementary Table 1). The supercomposite sample yielded a $\delta^{238}U$ of −0.170‰ ± 0.026‰. In addition to the composite samples we analysed three single samples from different depths: (1) a capping alkali basalt (−0.333‰ ± 0.044‰) from ~26 m above the 'start composite depth' of the altered crust section; (2) an altered MORB (−0.341‰ ± 0.044‰) in the upper composite section (~−100 m); and (3) a calcitic breccia (−0.114‰ ± 0.044‰) from the lowest composite zone (~−320 m). The differences in $\delta^{238}U$ between the latter two, normal, individual altered oceanic crust samples are reassuringly consistent with the composites, with the shallower sample showing significantly lower $\delta^{238}U$ than the deeper one. The alkali basalt sample has a high U content (0.7 p.p.m.), presumably reflecting its primary composition, which will be much less influenced by secondary U addition than MORB. Alkaline volcanism is atypical of oceanic crust stratigraphy but is a feature of some West Pacific drill sites, believed to be part of the burst of plume volcanism in the Cretaceous[25]. Fittingly, this alkali basalt sample has a $\delta^{238}U$ similar to other OIB (Supplementary Table 1).

The variable $\delta^{238}U$, at values distinct from seawater, shows that the seawater-derived U is not quantitatively incorporated during alteration in the ODP Site 801 AOC. During U uptake involving no redox transition, U isotopes generally appear to yield similar or slightly lower $\delta^{238}U$ values[16,17,26,63,70]. However, during the U(VI) to U(IV) reduction process U isotope fractionation is governed by both the nuclear field shift and mass-dependent mechanisms[71,72]. These processes lead to U isotope fractionation, but in opposite directions, with the nuclear field shift dominating the total observed $^{238}U/^{235}U$ fractionation and leading to a preference for the heavy isotope in the reduced immobile U(IV) form[18,19,71,72]. Such shifts towards higher $\delta^{238}U$, during redox-driven U uptake, have been documented in natural environments including U-enriched reducing sediments[17,37,63] and redox-driven roll-front U ore deposits[27,73,74]. With mass balance considerations in mind, it is clear that the U incorporation constitutes a partial reduction process, because a complete reduction of the available U would result in no net isotopic fractionation. This implies a process in which U is partitioned between U(VI) and U(IV) species but only the latter is fixed, and left immobile, with the former being transported away in the percolating fluid. Such a loss of isotopically light U during a partial U reduction process preferentially taking up heavy U isotopes has been shown in groundwaters associated with roll-front U ore deposits[73], *in situ* bio-stimulated U reduction flow-through experiments[75] and the anoxic Black Sea water column[76].

For the AOC at ODP Site 801, the $\delta^{238}U$ lower than the seawater composition in the upper 100 m may be expected from a dominant oxic U uptake, through adsorption, consistent with relatively oxidized conditions and high water/rock ratios[62]. A change to higher $\delta^{238}U$ in the lower part of the AOC is in accordance with general U addition through a reductive process and a U(VI)-to-U(IV) transition in the deeper part of the AOC with more restricted seawater flow-through[62,64]. Furthermore, the loss of isotopically light U to the upper part of the crust will mean that fluids percolating deeper may anyway have higher $\delta^{238}U$ signatures than the seawater composition. Both the lower and the middle part of the altered mafic crust have $\delta^{238}U$ higher than seawater, with the highest $\delta^{238}U$ found in the middle part. This observation may be related to the basement structure at ODP Site 801, with variable permeability and, hence, through-flow of seawater[62] and, consequently, heterogeneous U addition throughout the AOC. From the deposition of brown oxic haloes throughout the ODP Site 801 AOC, most oxic seawater through-flow has been estimated to occur in the upper 150 m and below 300 m depth in the core[62], and, consequently, the most reducing conditions are in between. This may explain why the highest $\delta^{238}U$ is found in the middle part, as U incorporated through U reduction is more dominant in this zone, compared to U uptake from oxic adsorption in the upper and lower sections.

Strikingly, the measured $\delta^{238}U$ and the U concentrations are very similar for the least-altered (FLO) and most-altered (VCL) material in each of the composite sections. This suggests that it is not the degree of alteration that dictates the U incorporation, but the ambient conditions. The relatively high $\delta^{238}U$ of the supercomposite suggests that the reduced U in the deeper part of the AOC dominates the overall $\delta^{238}U$ signature.

Assuming that such roll-front redox U uptake, as seen in the ODP Site 801 AOC, is representative of modern AOC U uptake and represents the integrated modern AOC for subduction, it delivers a high $\delta^{238}U$ to the mantle. In more reduced conditions U is expected to be taken up more quantitatively, resulting in little net isotopic fractionation of the added U. Such a scenario may be expected to describe the alteration of mafic oceanic crust from the percolation of anoxic seawater which dominated the deeper ocean before the second rise in atmospheric oxygen ~600 Myr ago[15,77]. This scenario would suggest insignificant U isotopic fractionation for U uptake into AOC before ~600 Myr ago, yielding a $\delta^{238}U$ similar to the mean $\delta^{238}U$ composition of rivers, the major U input into the ocean. At present, the best estimate of the modern riverine $\delta^{238}U$ flux to the ocean is −0.24‰ (ref. 78), close to our bulk Earth estimate. This suggests that U is released near-congruently with little net U isotope fractionation during oxidative terrestrial weathering and riverine transport. Assuming near-congruent U release during terrestrial weathering since the GOE ~2.4 Gyr ago, and oxidation of the atmosphere, quantitative uptake of U into the AOC would then imply a $\delta^{238}U$ composition near bulk Earth in the period ~2.4 Gyr to ~600 Myr ago.

Th–U–Pb systematics of OIB. The database. Our simple model of U recycling predicts that samples derived from increasingly young mantle sources will have increasingly subchondritic Th/U. To test this prediction we compiled data from the literature for samples, which have been analysed for both Th and U concentrations and Pb isotope compositions (Extended Data Table 1). The latter provide model age constraints, as detailed below.

To minimize the effects of analytical problems and secondary weathering processes obscuring primary signatures, we placed quite selective criteria for inclusion of samples into the data set, as follows.

(1) We included only samples with mass-spectrometric isotope dilution data on Th and U concentrations, coupled with U-series disequilibrium data. This ensures high-precision Th/U data and provides additional information on the magnitude of possible perturbation by the melting process (see below). Moreover, because samples collected for U-series data are all young, this also guards against U perturbation during weathering. As discussed above, mobility of U during weathering is otherwise a significant concern.

(2) We have selected only data from the main, shielding-building phases of islands. Later, post-erosional lavas are frequently invoked to contain a lithospheric component[79,80], and thus do not reflect the deep source we seek to investigate.

(3) In cases where several data sets exist for the sample location, we select the one containing the techniques more likely to be robust. Thus, in the case of the Azores, we use the data from ref. 81 rather than ref. 82, because the MC-ICPMS Pb data of the former provide much less-scattered model ages than those obtained from TIMS measurements of the latter.

Our database (Extended Data Table 1) thus comprises analyses from Hawaii, Iceland, Canary Islands (La Palma), Azores (Pico and São Miguel), Society Islands and Samoa. We also include a composite data point for Réunion derived from separate U-series and Pb isotope studies of historic eruptions. Although these studies are dominantly on different sample suites, the well-documented, extreme isotopic homogeneity of historic Réunion magmatism[83] gives us the confidence to combine the mean values of Th/U and Pb isotopes. There is one island (Pitcairn) for which appropriate data exists according to our criteria, but which we have not plotted for the following practical reasons. The very unradiogenic Pb isotope ratios of this island yields negative model ages in our calculations and so cannot be plotted together with the other data. This, combined with their extremely high Th/U, suggests that additional processes are responsible for the striking characteristics of this EMI-type composition, for example the erosion of deep continental crust[84]. In all, our compiled OIB database covers a similarly wide range of isotopic characteristics as represented by samples analysed for $\delta^{238}U$ (Fig. 1), and so forms a fitting complement.

In Fig. 3 we plot each individual datum from our compilation as a point, to show the range of compositions. To emphasize the contrasting mean compositions of different islands we have also averaged individual samples from a given island. A comment is required about the averaging of the Azores samples. The island of São Miguel has a marked spatial isotopic heterogeneity, with a distinct geographic (west-to-east) variation. Thus, we have added samples from the western volcanic centre (Sete Cidades) to the Pico samples to represent 'normal' Azores (I) while the other, more easterly samples are averaged to give 'enriched' Azores (II).

Pb model ages. It has long been known that a slope on the plot of $^{206}Pb/^{204}Pb$ versus $^{207}Pb/^{204}Pb$ potentially has age significance (see, for example, ref. 85). This approach was used to some effect in ref. 10, using the linear arrays in $^{206}Pb/^{204}Pb$ versus $^{207}Pb/^{204}Pb$ defined by some OIBs to calculate isochron ages of their sources, which ranged from 1 to 2.5 Gyr. Here we follow a similar approach. However, we did not want to rely on islands yielding well-defined linear arrays in Pb isotope space. Instead, we calculate the model ages of individual points rather than the slope of an array of data. Both approaches assume a common first stage for all samples. From this evolving reservoir a secondary model age (t_m) and U/Pb (μ_2) are calculated to produce the modern Pb isotopic composition. The parameters of our first-stage evolution are given in Extended Data Table 2 together with other input values.

The Pb model age we calculate represents an event that increased U/Pb to generate modern Pb isotopic compositions that lie to the right of the geochron. As discussed widely (see, for example, ref. 86), the process of subduction provides an appealing physical manifestation of this model scenario. During subduction, dehydration preferentially removes Pb from the mafic crust[87], increasing the U/Pb and Th/Pb of the deep subducted residue. Thus, we believe that the model ages relate to the time of subduction of recycled oceanic crust found in OIB sources.

Explicitly, we calculate our model ages by rearranging and numerically solving the following two equations (1) and (2) for μ_2 and t_M (using parameters described in Extended Data Table 2):

$$\frac{^{206}Pb}{^{204}Pb} = \frac{^{206}Pb}{^{204}Pb_{CD}} + \mu_1\left(e^{\lambda_{238}t} - e^{\lambda_{238}t_m}\right) + \mu_2\left(e^{\lambda_{238}t_m} - 1\right) \quad (1)$$

$$\frac{^{207}Pb}{^{204}Pb} = \frac{^{207}Pb}{^{204}Pb_{CD}} + \frac{\mu_1}{137.88}\left(e^{\lambda_{235}t} - e^{\lambda_{235}t_m}\right) + \frac{\mu_2}{137.88}\left(e^{\lambda_{235}t_m} - 1\right) \quad (2)$$

Having obtained μ_2 and t_M a model Th/U (weight ratio) of the second stage may then be calculated accordingly by rearranging equation (3):

$$\frac{^{208}Pb}{^{204}Pb} = \frac{^{208}Pb}{^{204}Pb_{CD}} + \frac{Th}{U_1}k\mu_1\left(e^{\lambda_{232}t} - e^{\lambda_{232}t_m}\right) + \frac{Th}{U}k\mu_2\left(e^{\lambda_{232}t_m} - 1\right) \quad (3)$$

Extended Data Table 1 contains the averaged, calculated model Pb ages for our OIB data set, whereas the individual model Pb ages versus measured Th/U and modelled Th/U (Pb, two-stage) are shown in Fig. 3. We use Th/U (weight ratio) throughout as this is most commonly reported in the literature, although $^{232}Th/^{238}U$ (atomic ratio, κ) is required in the calculations (the difference between these two ratios is not great). The measured Th/U is potentially perturbed by melting or during melt migration to the surface, or both. For this reason, we used only samples for which U-series measurements were available, which provides direct constraints on the magnitude of this process. All samples in our data set have ^{230}Th excesses, from 1% to 37% (Extended Data Fig. 3). This implies no more than a 37% increase in Th/U during melt generation and likely less (see, for example, the discussion in ref. 88). As in the case of MORB, recent melting cannot explain the trend to lower Th/U from values close to the planetary reference (3.876).

The Samoan samples are notable for having Th/U higher (4.0–5.3) than the planetary reference value. This cannot be solely a result of recent melt fractionation because these samples have minor ($^{230}Th/^{238}U$) disequilibrium (Extended Data Fig. 3). This high Th/U is potentially associated with lithospheric enrichment from plume-derived carbonatitic metasomatism, which can fractionate Th/U but will not influence the Pb isotopes[89]. We note that the Samoan Pb isotopes are incompatible with their high Th/U being associated with ancient fractionation; that is, they have model Th/U within error of the planetary Th/U. Although the Samoan source has long been associated with recycled continental sediments[90], if these were recycled before the major rise in atmospheric oxygen (as is compatible with their model ages), then the Th/U of the continental material should be unfractionated[91,92]. Consequently, whether or not the enriched component is continental is not a critical issue. We also stress that the overall trend in Fig. 3 is not pinned by Samoa, but includes Réunion and the enriched samples of São Miguel. For the latter, there has been a detailed discussion of why recycled sediment is not implicated in this source[28].

The apparently continuously declining Th/U of OIBs and their typically higher values than MORB argues against excess U left residual in the subducting slab having a significant role in lowering Th/U of OIBs. Rather, we infer that the slab adds its excess U, from sea-floor alteration, to the upper mantle. As hypothesized in the main text this is likely to result from its mineralogical host becoming unstable during pro-grade metamorphism. A host such as allanite[29] would survive beyond the subduction zone, but would ultimately melt to transfer U into the surrounding mantle. Thus, we infer that the declining Th/U of OIBs reflects the steadily decreasing Th/U of the upper-mantle source, which forms crust subsequently recycled to produce further OIBs. In this model, the upper mantle always has lower Th/U than previously formed OIB sources. The need for the excess U to be lost from recycled oceanic crust has also been discussed in terms of the Pb isotope systematics of OIB (see, for example, refs 93, 94).

31. Gutjahr, M. *et al.* Reliable extraction of a deepwater trace metal isotope signal from Fe–Mn oxyhydroxide coatings of marine sediments. *Chem. Geol.* **242,** 351–370 (2007).
32. Goldstein, S. J., Murrell, M. T. & Janecky, D. R. Th and U isotopic systematics of basalts from the Juan de Fuca and Gorda Ridges by mass spectrometry. *Earth Planet. Sci. Lett.* **96,** 134–146 (1989).
33. Bourdon, B., Goldstein, S. J., Bourles, D., Murrell, M. T. & Langmuir, C. H. Evidence from ^{10}Be and U series disequilibria on the possible contamination of mid-ocean ridge basalt glasses by sedimentary material. *Geochem. Geophys. Geosyst.* **1,** 2000GC000047 (2000).
34. Reinitz, I. & Turekian, K. K. $^{230}Th/^{238}U$ and $^{226}Ra/^{230}Th$ fractionation in young basaltic glasses from the East Pacific Rise. *Earth Planet. Sci. Lett.* **94,** 199–207 (1989).
35. Andersen, M. B., Vance, D., Keech, A. R., Rickli, J. & Hudson, G. Estimating U fluxes in a high-latitude, boreal post-glacial setting using U-series isotopes in soils and rivers. *Chem. Geol.* **354,** 22–32 (2013).
36. Richter, S. *et al.* The isotopic composition of natural uranium samples—Measurements using the new $^{233}U/^{236}U$ double spike IRMM-3636. *Int. J. Mass Spectrom.* **269,** 145–148 (2008).
37. Andersen, M. B. *et al.* A modern framework for the interpretation of $^{238}U/^{235}U$ in studies of ancient ocean redox. *Earth Planet. Sci. Lett.* **400,** 184–194 (2014).
38. Hiess, J., Condon, D. J., McLean, N. & Noble, S. R. $^{238}U/^{235}U$ systematics in terrestrial uranium-bearing minerals. *Science* **335,** 1610–1614 (2012).
39. Russell, W. A., Papanastassiou, D. & Tombrello, T. A. Ca isotope fractionation on the Earth and other solar system materials. *Geochim. Cosmochim. Acta* **42,** 1075–1090 (1978).
40. Cheng, H. *et al.* Improvements in ^{230}Th dating, ^{230}Th and ^{234}U half-life values, and U–Th isotopic measurements by multi-collector inductively coupled plasma mass spectrometry. *Earth Planet. Sci. Lett.* **371–372,** 82–91 (2013).
41. Steele, R. C. J., Elliott, T., Coath, C. D. & Regelous, M. Confirmation of mass-independent Ni isotopic variability in iron meteorites. *Geochim. Cosmochim. Acta* **75,** 7906–7925 (2011).

42. Stirling, C. H., Halliday, A. N. & Porcelli, D. In search of live ^{247}Cm in the early solar system. *Geochim. Cosmochim. Acta* **69,** 1059–1071 (2005).
43. Stirling, C. H., Halliday, A. N., Potter, E.-K., Andersen, M. B. & Zanda, B. A low initial abundance of ^{247}Cm in the early solar system: implications for r-process nucleo-synthesis. *Earth Planet. Sci. Lett.* **251,** 386–397 (2006).
44. Brennecka, G. A. & Wadhwa, M. Uranium isotope compositions of the basaltic angrite meteorites and the chronological implications for the early Solar System. *Proc. Natl Acad. Sci. USA* **109,** 9299–9303 (2012).
45. Brennecka, G. A. *et al.* ^{238}U/^{235}U variations in meteorites: extant ^{247}Cm and implications for Pb-Pb dating. *Science* **327,** 449–451 (2010).
46. Amelin, Y. *et al.* U–Pb chronology of the Solar System's oldest solids with variable ^{238}U/^{235}U. *Earth Planet. Sci. Lett.* **300,** 343–350 (2010).
47. Rocholl, A. & Jochum, K. P. Th, U and other trace-elements in carbonaceous chondrites: implications for the terrestrial and solar-system Th/U ratios. *Earth Planet. Sci. Lett.* **117,** 265–278 (1993).
48. Dauphas, N., Marty, B. & Reisberg, L. Molybdenum evidence for inherited planetary scale isotope heterogeneity of the protosolar nebula. *Astrophys. J.* **565,** 640–644 (2002).
49. Trinquier, A. *et al.* Origin of nucleosynthetic isotope heterogeneity in the solar protoplanetary disk. *Science* **324,** 374–376 (2009).
50. Barrat, J. A. *et al.* The Stannern trend eucrites: contamination of main group eucritic magmas by crustal partial melts. *Geochim. Cosmochim. Acta* **71,** 4108–4124 (2007).
51. Morgak, J. W. & Lovering, J. F. Uranium and thorium in achondrites. *Geochim. Cosmochim. Acta* **37,** 1697–1707 (1973).
52. Manhès, G., Allègre, C. J. & Provost, A. U-Th-Pb systematics of the eucrite ''Juvinas'': precise age determination and evidence for exotic lead. *Geochim. Cosmochim. Acta* **48,** 2247–2264 (1984).
53. Zindler, A. & Hart, S. Chemical geodynamics. *Annu. Rev. Earth Planet. Sci.* **14,** 493–571 (1986).
54. Hart, S. R., Hauri, E. H., Oschmann, L. A. & Whitehead, J. A. Mantle plumes and entrainment: isotopic evidence. *Science* **256,** 517–520 (1992).
55. Farley, K. A. & Neroda, E. Noble gases in the Earth's mantle. *Annu. Rev. Earth Planet. Sci.* **26,** 189–218 (1998).
56. Sims, K. W. W. *et al.* Chemical and isotopic constraints on the generation and transport of magma beneath the East Pacific Rise. *Geochim. Cosmochim. Acta* **66,** 3481–3504 (2002).
57. Waters, C. L. *et al.* Recent volcanic accretion at 9° N–10° N East Pacific Rise as resolved by combined geochemical and geological observations. *Geochem. Geophys. Geosyst.* **14,** 2547–2574 (2013).
58. Regelous, M. *et al.* Variations in the geochemistry of magmatism on the East Pacific Rise at 10 30′ N since 800 ka. *Earth Planet. Sci. Lett.* **168,** 45–63 (1999).
59. Regelous, M., Niu, Y., Abouchami, W. & Castillo, P. R. Shallow origin for South Atlantic Dupal Anomaly from lower continental crust: geochemical evidence from the Mid-Atlantic Ridge at 26 S. *Lithos* **112,** 57–72 (2009).
60. Robinson, C. J., White, R. S., Bickle, M. J. & Minshull, T. A. Restricted melting under the very slow-spreading Southwest Indian Ridge. *Geol. Soc. Lond. Spec. Publ.* **118,** 131–141 (1996).
61. Avanzinelli, R. *et al.* Combined ^{238}U/^{230}Th and ^{235}U/^{231}Pa constraints on the transport of slab-derived material beneath the Mariana Islands. *Geochim. Cosmochim. Acta* **92,** 308–328 (2012).
62. Alt, J. C. & Teagle, D. A. Hydrothermal alteration of upper oceanic crust formed at a fast-spreading ridge: mineral, chemical, and isotopic evidence from ODP Site 801. *Chem. Geol.* **201,** 191–211 (2003).
63. Romaniello, S. J., Herrmann, A. D. & Anbar, A. D. Uranium concentrations and ^{238}U/^{235}U isotope ratios in modern carbonates from the Bahamas: assessing a novel paleoredox proxy. *Chem. Geol.* **362,** 305–316 (2013).
64. Alt, J. C, *et al.* Subsurface structure of a submarine hydrothermal system in ocean crust formed at the East Pacific Rise, ODP/IODP Site 1256. *Geochem. Geophys. Geosyst.* **11,** 2010GC003144 (2010).
65. Staudigel, H. Hydrothermal alteration processes in the oceanic crust. *Treatise Geochem.* **3,** 511–535 (2003).
66. Chen, J., Wasserburg, G., Von Damm, K. & Edmond, J. The U-Th-Pb systematics in hot springs on the East Pacific Rise at 21 N and Guaymas Basin. *Geochim. Cosmochim. Acta* **50,** 2467–2479 (1986).
67. Mottl, M. *et al.* Warm springs discovered on 3.5 Ma oceanic crust, eastern flank of the Juan de Fuca Ridge. *Geology* **26,** 51–54 (1998).
68. Plank, T. *et al. Proc. Ocean Drilling Program, Initial Reports* Vol. 185 (Ocean Drilling Program, 2000).
69. Staudigel, H., Plank, T., White, B. & Schmincke, H.-U. Geochemical fluxes during seafloor alteration of the basaltic upper oceanic crust: DSDP Sites 417 and 418. *Geophys. Monogr. Ser.* **96,** 19–38 (1996).
70. Shiel, A. E. *et al.* No measurable changes in ^{238}U/^{235}U due to desorption–adsorption of U(VI) from groundwater at the Rifle, Colorado, integrated field research challenge site. *Environ. Sci. Technol.* **47,** 2535–2541 (2013).
71. Bigeleisen, J. Nuclear size and shape effects in chemical reactions. Isotope chemistry of heavy elements. *J. Am. Chem. Soc.* **118,** 3676–3680 (1996).
72. Fujii, Y., Higuchi, N., Haruno, Y., Nomura, M. & Suzuki, T. Temperature dependence of isotope effects in uranium chemical exchange reactions. *J. Nucl. Sci. Technol.* **43,** 400–406 (2006).
73. Murphy, M. J., Stirling, C. H., Kaltenbach, A., Turner, S. P. & Schaefer, B. F. Fractionation of ^{238}U/^{235}U by reduction during low temperature uranium mineralisation processes. *Earth Planet. Sci. Lett.* **388,** 306–317 (2014).
74. Brennecka, G. A., Borg, L. E., Hutcheon, I. D., Sharp, M. A. & Anbar, A. D. Natural variations in uranium isotope ratios of uranium ore concentrates: understanding the ^{238}U/^{235}U fractionation mechanism. *Earth Planet. Sci. Lett.* **291,** 228–233 (2010).
75. Bopp, C. J., IV *et al.* Uranium ^{238}U/^{235}U isotope ratios as indicators of reduction: results from an in situ biostimulation experiment at Rifle, Colorado, USA. *Environ. Sci. Technol.* **44,** 5927–5933 (2010).
76. Romaniello, S. J., Brennecka, G. A., Anbar, A. D. & Colman, A. S. Natural isotopic fractionation of ^{238}U/^{235}U in the water column of the Black Sea. *Eos Trans. AGU* **90, 52,** V54C–06 (2009).
77. Partin, C. A. *et al.* Large-scale fluctuations in Precambrian atmospheric and oceanic oxygen levels from the record of U in shales. *Earth Planet. Sci. Lett.* **369-370,** 284–293 (2013).
78. Noordmann, J. *et al.* Fractionation of ^{238}U/^{235}U during weathering and hydrothermal alteration. *Mineral. Mag.* **76,** A1548 (2012).
79. Class, C. & Goldstein, S. L. Plume-lithosphere interactions in the ocean basins: constraints from the source mineralogy. *Earth Planet. Sci. Lett.* **150,** 245–260 (1997).
80. Lundstrom, C., Hoernle, K. & Gill, J. U-series disequilibria in volcanic rocks from the Canary Islands: plume versus lithospheric melting. *Geochim. Cosmochim. Acta* **67,** 4153–4177 (2003).
81. Elliott, T., Blichert-Toft, J., Heumann, A., Koetsier, G. & Forjaz, V. The origin of enriched mantle beneath Sao Miguel, Azores. *Geochim. Cosmochim. Acta* **71,** 219–240 (2007).
82. Turner, S., Hawkesworth, C., Rogers, N. & King, P. U-Th isotope disequilibria and ocean island basalt generation in the Azores. *Chem. Geol.* **139,** 145–164 (1997).
83. Graham, D., Lupton, J., Albarède, F. & Condomines, M. Extreme temporal homogeneity of helium-isotopes at Piton-De-La-Fournaise, Réunion Island. *Nature* **347,** 545–548 (1990).
84. Willbold, M. & Stracke, A. Trace element composition of mantle endmembers: implications for recycling of oceanic and upper and lower continental crust. *Geochem. Geophys. Geosyst.* **7,** 2005GC001005 (2006).
85. Patterson, C. C. Age of meteorites and the Earth. *Geochim. Cosmochim. Acta* **10,** 230–237 (1956).
86. Chauvel, C., Lewin, E., Carpentier, M., Arndt, N. T. & Marini, J.-C. Role of recycled oceanic basalt and sediment in generating the Hf–Nd mantle array. *Nature Geosci.* **1,** 64–67 (2008).
87. Miller, D. M., Goldstein, S. L. & Langmuir, C. H. Cerium/lead and lead isotope ratios in arc magmas and the enrichment of lead in the continents. *Nature* **368,** 514–520 (1994).
88. Elliott, T. Fractionation of U and Th during mantle melting: a reprise. *Chem. Geol.* **139,** 165–183 (1997).
89. Hauri, E. H., Shimizu, N., Dieu, J. J. & Hart, S. R. Evidence for hotspot-related carbonatite metasomatism in the oceanic upper mantle. *Nature* **365,** 221–227 (1993).
90. Wright, E. & White, W. M. The origin of Samoa: new evidence from Sr, Nd, and Pb isotopes. *Earth Planet. Sci. Lett.* **81,** 151–162 (1987).
91. McLennan, S. M. & Taylor, S. R. Th and U in sedimentary rocks: crustal evolution and sedimentary recycling. *Nature* **285,** 621–624 (1980).
92. Jackson, M. G. *et al.* The return of subduction continental crust in Samoan lavas. *Nature* **448,** 684–687 (2007).
93. Staudigel, H. & Hart, S. R. Alteration of basaltic glass: mechanisms and significance for the oceanic crust-seawater budget. *Geochim. Cosmochim. Acta* **47,** 337–350 (1983).
94. Chauvel, C., Hofmann, A. W. & Vidal, P. HIMU-EM: the French Polynesian connection. *Earth Planet. Sci. Lett.* **110,** 99–119 (1992).
95. Pietruszka, A. J. & Garcia, M. O. The size and shape of Kilauea Volcano's summit magma storage reservoir: a geochemical probe. *Earth Planet. Sci. Lett.* **167,** 311–320 (1999).
96. Sims, K. W. W. *et al.* Mechanisms of magma generation beneath Hawaii and mid-ocean ridges: uranium/thorium and samarium/neodymium isotopic evidence. *Science* **267,** 508–512 (1995).
97. Sims, K. W. W. *et al.* Porosity of the melting zone and variations in the solid mantle upwelling rate beneath Hawaii: inferences from ^{238}U- ^{230}Th-^{226}Ra and ^{235}U-^{231}Pa disequilibria. *Geochim. Cosmochim. Acta* **63,** 4119–4138 (1999).
98. Kokfelt, T. F. *et al.* Combined trace element and Pb-Nd–Sr-O isotope evidence for recycled oceanic crust (upper and lower) in the Iceland mantle plume. *J. Petrol.* **47,** 1705–1749 (2006).
99. Kokfelt, T. F., Hoernle, K. & Hauff, F. Upwelling and melting of the Iceland plume from radial variation of ^{238}U-^{230}Th disequilibria in postglacial volcanic rocks. *Earth Planet. Sci. Lett.* **214,** 167–186 (2003).
100. Prytulak, J. & Elliott, T. Determining melt productivity of mantle sources from ^{238}U-^{230}Th and ^{235}U–^{231}Pa disequilibria; an example from Pico Island, Azores. *Geochim. Cosmochim. Acta* **73,** 2103–2122 (2009).
101. Prytulak, J. *et al.* Melting versus contamination effects on ^{238}U-^{230}Th-^{226}Ra and ^{235}U-^{231}Pa disequilibria in lavas from Sao Miguel, Azores. *Chem. Geol.* **381,** 94–109 (2014).
102. Elliott, T. *Element Fractionation in the Petrogenesis of Ocean Island Basalts* 29–92. PhD thesis, Open Univ. (1991).
103. Marcantonio, F., Zindler, A., Elliott, T. & Staudigel, H. Os isotope systematics of La Palma, Canary Islands: evidence for recycled crust in the mantle source of HIMU ocean islands. *Earth Planet. Sci. Lett.* **133,** 397–410 (1995).
104. Hémond, C., Devey, C. W. & Chauvel, C. Source compositions and melting processes in the Society and Austral plumes (South Pacific Ocean): element and isotope (Sr, Nd, Pb, Th) geochemistry. *Chem. Geol.* **115,** 7–45 (1994).
105. Sims, K. W. W. & Hart, S. R. Comparison of Th, Sr, Nd and Pb isotopes in oceanic basalts: implications for mantle heterogeneity and magma genesis. *Earth Planet. Sci. Lett.* **245,** 743–761 (2006).

106. Bosch, D. *et al*. Pb, Hf and Nd isotope compositions of the two Réunion volcanoes (Indian Ocean): a tale of two small-scale mantle ''blobs''? *Earth Planet. Sci. Lett.* **265,** 748–765 (2008).

107. Sigmarsson, O., Condomines, M. & Bachèlery, P. Magma residence time beneath the Piton de la Fournaise Volcano, Reunion Island, from U-series disequilibria. *Earth Planet. Sci. Lett.* **234,** 223–234 (2005).

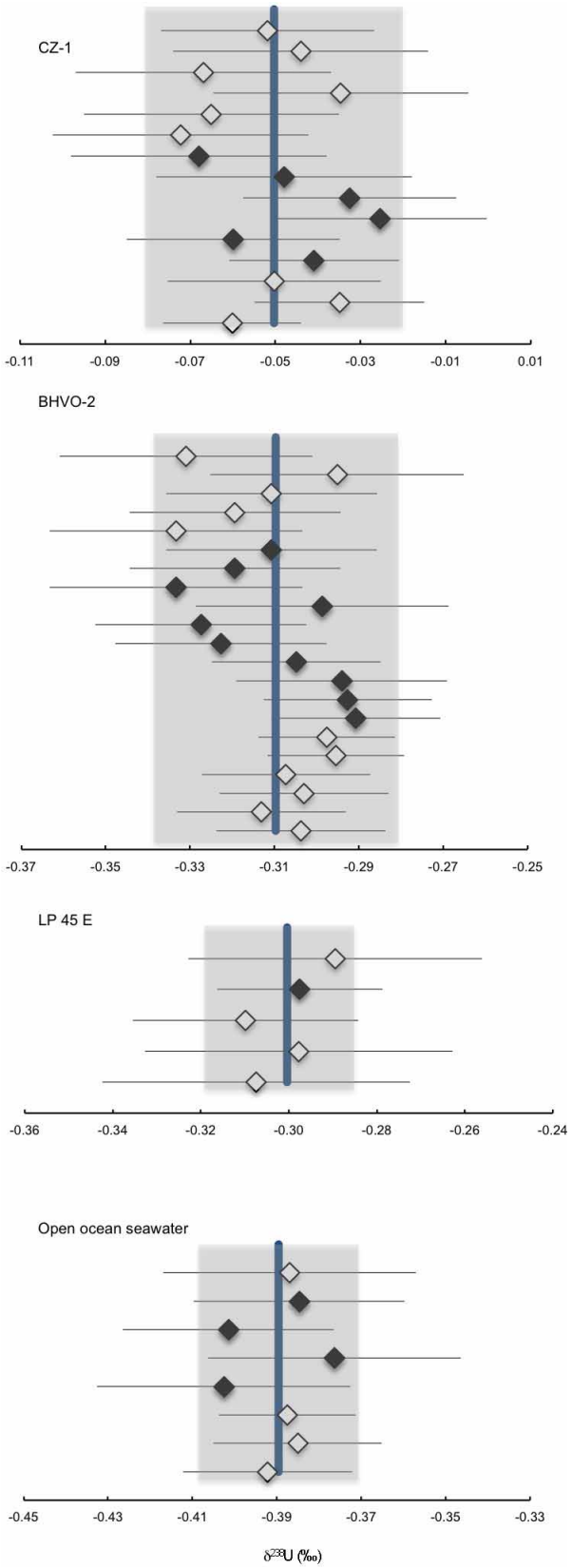

Extended Data Figure 1 | $\delta^{238}U$ reproducibility of standards. Repeated $\delta^{238}U$ measurements of a range of standards with different matrixes (CZ-1 uraninite, BHVO-2/LP 45 E basalts, seawater) are shown. All have external reproducibility (2 s.d., grey shaded area) better than ±0.30‰, a similar range to the internal measurement uncertainty (2 s.e.) for individual samples (Methods). The different symbols refer to the different measurement set-ups (Supplementary Table 4).

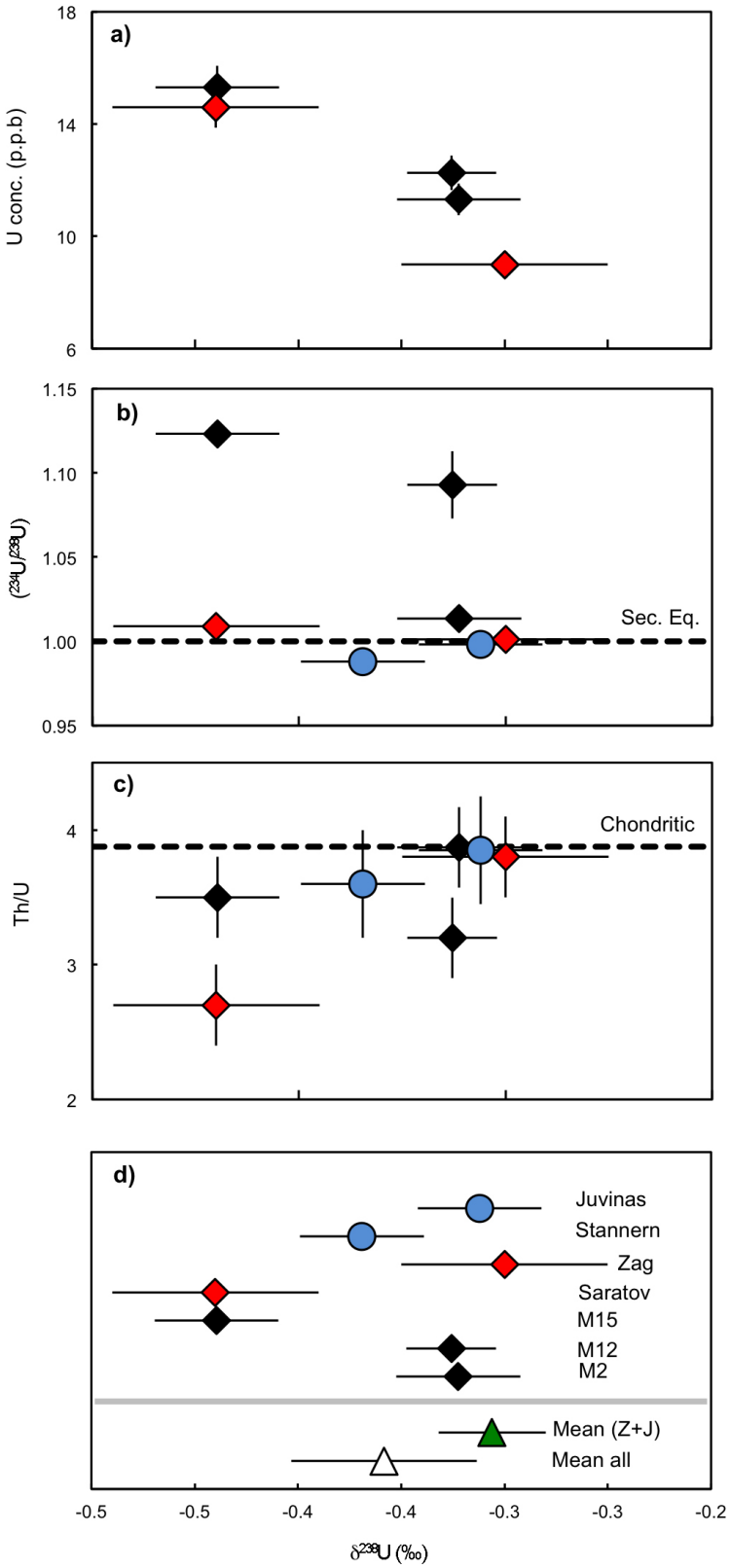

Extended Data Figure 2 | U–Th geochemistry of analysed meteorites. **a**, $\delta^{238}U$ versus U concentration for ordinary chondrites (black diamonds, 'finds'; red diamonds, 'falls'). **b**, $\delta^{238}U$ versus ($^{234}U/^{238}U$) for ordinary chondrites (symbols as in **a**) and eucrites (blue circles). **c**, $\delta^{238}U$ versus Th/U for the same samples as in **a** and **b**. **d**, A 'Caltech plot' of the $\delta^{238}U$ of individual meteorite samples and averages based on (1) the only two meteorites with ($^{234}U/^{238}U$) within error of secular equilibrium ('Mean (Z+J)') and (2) all of the analysed meteorites ('Mean all'). Error bars denote 2 s.e.m.

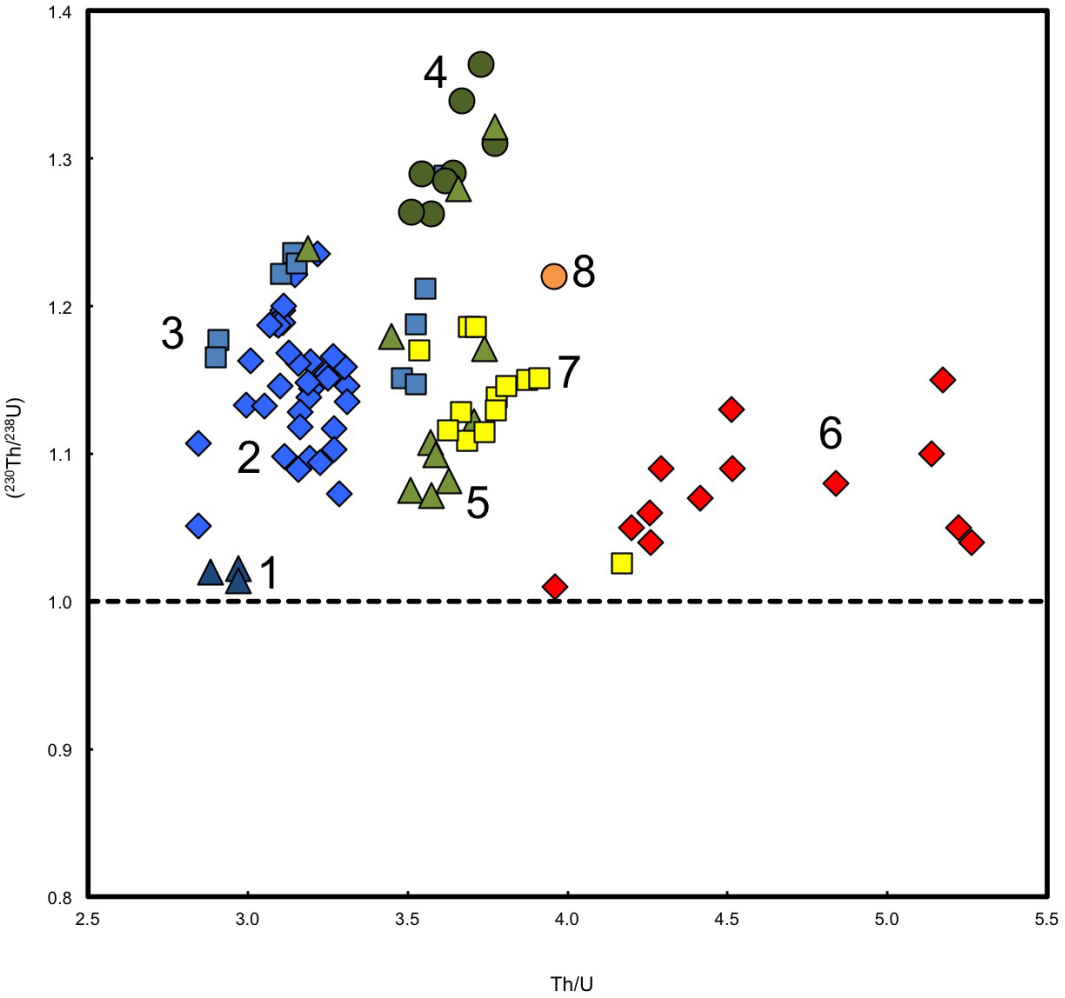

Extended Data Figure 3 | U–Th isotope systematics in the OIB used for Pb age modelling. Symbol colours are as in Fig. 3: (1) Hawaii, (2) Iceland, (3) Azores I, (4) La Palma, (5) French Polynesia, (6) Samoa, (7) Azores II, (8) Réunion. References can be found in Extended Data Table 1. Note that the *y* axis shows activity ratio whereas the *x* axis shows a weight ratio. The dashed line represents secular equilibrium of (^{230}Th/^{238}U).

Extended Data Table 1 | Literature compilation of Pb, U and Th in Ocean Island Basalts

N*	Locality	Ref. Pb	Ref. Th/U	n†	age (Ga)‡
1.	Hawaii (Kilaeua)	(95,96,97)	(95,96,97)	3	1.76
2.	Iceland	(98)	(99)	35	1.81
3.	Azores I (São Miguel/Pico)	(81)	(100,101)	10	1.89
4.	Canaries (La Palma)	(102,103)	(102)	8	1.92
5.	French Polynesia	(104)	(104)	11	2.12
6.	Samoa	(105)	(105)	13	2.25
7.	Azores II (São Miguel)	(81)	(100)	13	2.33
8.	Rèunion	(106)	(107)	(average)	2.42

*Locality number used in main text Figure 3

†Number of individual data-points

‡ Average Pb model ages (t_m) for each locality, see methods

Extended Data Table 2 | Input parameters for calculating Pb model ages

Initial composition:*	
$^{206}Pb/^{204}Pb$ *(Canyon Diablo)*:	9.3066
$^{207}Pb/^{204}Pb$ *(Canyon Diablo)*:	10.293
$^{208}Pb/^{204}Pb$ *(Canyon Diablo)*:	29.475
μ_1 (1. Stage $^{238}U/^{204}Pb$):	7.85
Th/U_1 (1. Stage):	3.876
t (time ago, Ga):	4.57
$^{238}U/^{235}U$:	137.88†
k:	1.03326‡
Decay constants (y^{-1}):	
λ_{238} (^{238}U):	1.551E-10
λ_{235} (^{235}U):	9.849E-10
λ_{232} (^{232}Th):	4.948E-11

*Radioactive element abundances and ratios are reported as present day values

†The "old consensus value" is used to be comparable with literature data

‡k is the conversion factor of Th/U weight ratios to atomic ratios of $^{232}Th/^{238}U$ (or kappa). We use Th/U (weight ratios) throughout the text for consistency with most literature